water

MDPI

Article

Assessment of Storm Surge Disaster Response Capacity in Chinese Coastal Cities Using Urban-Scale Survey Data

Li Zhu [1,2,*] and Shibai Cui [1]

[1] Department of Architecture, Tianjin University, Tianjin 300072, China; cuicuicui2006@163.com
[2] APEC Sustainable Energy Center, Tianjin 300072, China
* Correspondence: zhuli1977@tju.edu.cn; Tel.: +86-17743468411

Abstract

Currently, most studies evaluating storm surges are conducted at the provincial level, and there is a lack of detailed research focusing on cities. This paper focuses on the urban scale, using some fine-scale data of coastal areas obtained through remote sensing images. This research is based on the Hazard–Exposure–Vulnerability (H-E-V) framework and PPRR (Prevention, Preparedness, Response, and Recovery) crisis management theory. It focuses on 52 Chinese coastal cities as the research subject. The evaluation system for the disaster response capabilities of Chinese coastal cities was constructed based on three aspects: the stability of the disaster-incubating environment (S), the risk of disaster-causing factors (R), and the vulnerability of disaster-bearing bodies (V). The significance of this study is that the storm surge capability of China's coastal cities can be analyzed based on the results of the evaluation, and the evaluation model can be used to identify its deficiencies. In this paper, these storm surge disaster response capabilities of coastal cities were scored using the entropy weighted TOPSIS method and the weight rank sum ratio (WRSR), and the results were also analyzed. The results indicate that Wenzhou has the best comprehensive disaster response capability, while Yancheng has the worst. Moreover, Tianjin, Ningde, and Shenzhen performed well in the three aspects of vulnerability of disaster-bearing bodies, risk of disaster-causing factors, and stability of disaster-incubating environment separately. On the contrary, Dandong (tied with Qinzhou), Jiaxing, and Chaozhou performed poorly in the above three areas.

Keywords: storm surge; Chinese coastal cities; disaster response capacity; entropy weighted TOPSIS; grey relational analysis

check for updates

Academic Editor: Chin H Wu

Received: 30 June 2025
Revised: 21 July 2025
Accepted: 25 July 2025
Published: 28 July 2025

Citation: Zhu, L.; Cui, S. Assessment of Storm Surge Disaster Response Capacity in Chinese Coastal Cities Using Urban-Scale Survey Data. *Water* **2025**, *17*, 2245. https://doi.org/10.3390/w17152245

Copyright: © 2025 by the authors. Licensee MDPI, Basel, Switzerland. This article is an open access article distributed under the terms and conditions of the Creative Commons Attribution (CC BY) license (https://creativecommons.org/licenses/by/4.0/).

1. Introduction

Storm surge disasters (SSDs) are a common marine hazard along ocean coastlines, characterized by abnormal fluctuations in sea level caused by strong winds and rapid changes in atmospheric pressure. These events are typically triggered by typhoons and extratropical cyclones, which push seawater toward the shore. As a result, sea levels in affected areas can rise far above normal tidal ranges, leading to severe coastal flooding and infrastructure damage [1–4]. Across the globe, storm surges are widely acknowledged as critical coastal hazards that have caused substantial loss of life, economic disruption, and long-term social impacts. Events such as Hurricane Katrina in 2005 (USA) and Storm Xaver in 2013 (Northern Europe) have revealed how inadequate coastal planning and infrastructure can amplify disaster impacts. In response, countries like the Netherlands have

developed comprehensive flood defense systems through the integration of delta engineering and coastal zone governance, setting global benchmarks in surge resilience. Likewise, East Asian nations, such as Japan and South Korea, have implemented mixed strategies combining engineered defenses—like sea barriers—with nature-based approaches, including wetland conservation and restoration. These international approaches demonstrate the value of localized, city-scale disaster preparedness in enhancing resilience to storm surges. By contrast, most Chinese studies to date have focused on macro-scale evaluations, with insufficient attention given to differences in vulnerability and preparedness across individual coastal cities. According to 2020 data, China's coastline is 32,977.34 km long, and the cities that have a coastline are frequently impacted by SSDs due to their unique climate and geographic positioning [5,6]. The geographical positioning of China's coastline renders it susceptible to storm surges. These events have historically caused substantial human casualties and economic losses. Specifically, from 2000 to 2022, SSDs inflicted approximately $32 billion in economic damages and left 888 people missing or dead, while the development of the storm surge early-warning system has resulted in a significant reduction in these casualties. However, the human and economic losses caused by SSDs have increased significantly due to the rapid growth of both, coastal populations and economies [7]. This development highlights the complex interplay between technological advancements in disaster prediction and management, and the challenges posed by economic growth and demographic shifts in coastal areas.

Most contemporary research on SSDs in China focuses on storm surge warning forecasts, estimating the damage caused by storm surges, and assessing storm surge tide levels at different recurrence periods. Some of these studies particularly focus on coastal vulnerability and risk assessment. For example, Shi et al. developed a risk assessment method using the Shanghai area as a case study, and Huang et al. conducted a vulnerability assessment for Chinese coastal areas [3,8]. In disaster studies, the relationship between the disaster-bearing bodies and the cause of the disaster is usually extremely complex, and currently, few comprehensive studies regarding storm surges have been made that are based on the capability of the disaster-bearing bodies. Furthermore, research on the causative mechanisms of storm surges lacks systematicity, and future assessments of SSDs should focus on the refinement of current methodologies. Not only is it necessary to refine the types of losses, but it is also important to segment the objects and areas being evaluated. This assessment process should include a detailed delineation of the natural, social, economic, and environmental characteristics typical to a specific region. Currently, research on vulnerable entities based on SSDs is mainly focused on the provincial level, with a need for more research on the city level. Although Meng et al. conducted a similar vulnerability study that paid particular attention to the impact of storm surges on cities, only 30 coastal cities were included in that sample, meaning that more than 20 Chinese coastal prefecture-level cities were ignored in the results [5]. In the context of urban management concerning SSDs, scholars from various countries have conducted extensive research. Blankespoor et al. quantified the coastal protection services provided by mangroves in mitigating storm surges, underscoring the impact of mangrove loss on storm surge areas [9]. Nguyen et al. assessed storm surge risks in aquaculture in the Northern coastal area of Vietnam, providing a scientific basis for proactive response plans and policy-making to reduce storm surge damage [10]. Xu et al. investigated the joint risk of rainfall and storm surges during typhoons in a coastal city in China, providing insights for urban flood risk assessment and management [11]. However, their study lacks a comprehensive evaluation of coastal cities from multiple perspectives and in a holistic manner. The present study evaluates the prefecture-level cities along China's coastline from various perspectives and gives management advice.

A disaster is recognized when an event exceeds the response capability of the affected entity, highlighting the need for a thorough examination of its response capability. To clarify the current response capabilities of Chinese coastal cities to SSDs, this study presents the following approach. (1) Using the H-E-V framework, the disaster system functional system, and the integration of PPRR theory, a framework is developed to assess the disaster response capability (DRC) of coastal cities against storm surges. (2) This study employs the entropy weight TOPSIS method and the weight rank sum ratio (WRSR) method, in combination with the H-E-V framework, to calculate the DRC scores of coastal cities against storm surges. (3) Given the need for more in-depth research on response capability, this paper analyses the SSD response capability of urban disaster-bearing bodies in order to compare the differing response capacities of various cities to SSDs. The results of this research will be of great significance to the governmental bodies responsible for future urban development and emergency planning.

2. Study Area

China's coastline is characterized by a complex administrative composition that includes 9 coastal provincial regions (Taiwan inclusive), 1 autonomous region, 2 special administrative regions, 55 coastal provincial prefecture-level cities (excluding Hong Kong, Macao, and Taiwan), and 242 coastal districts and counties distributed along China's coastline. This paper is based on the context of Chinese districts, and adopts the city as the primary unit of analysis. A total of 54 provincial prefecture-level cities, excluding Hong Kong, Macao, Taiwan, and Sansha City, were initially included in the scope of this study.

Among these coastal cities, it is commonly accepted that the demarcation between the Qiantang River and Hangzhou Bay stretches from Haining Ganpu (part of Jiaxing) to the Yuyao Xisan Sluice (part of Ningbo). Thus, Hangzhou and Shaoxing are not considered coastal cities. Given that the eight estuaries of the Pearl River serve as the boundary between river and sea, Guangzhou and Dongguan are defined as coastal cities. At the same time, Sansha City, due to its minimal population, is temporarily excluded from this categorization. Following a rigorous selection process, this study identifies a cohort of 52 coastal cities (as depicted in Figure 1).

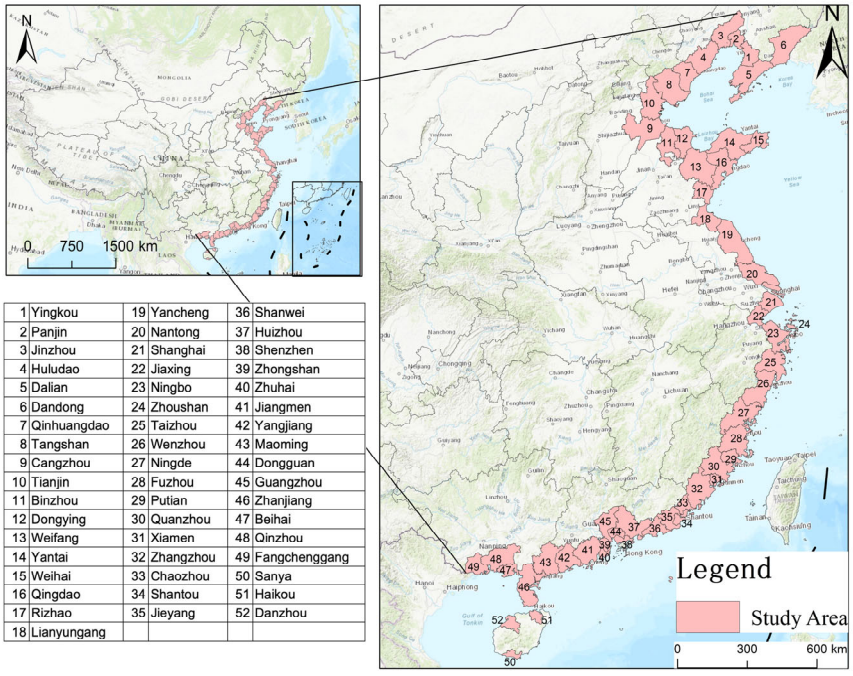

1	Yingkou	19	Yancheng	36	Shanwei
2	Panjin	20	Nantong	37	Huizhou
3	Jinzhou	21	Shanghai	38	Shenzhen
4	Huludao	22	Jiaxing	39	Zhongshan
5	Dalian	23	Ningbo	40	Zhuhai
6	Dandong	24	Zhoushan	41	Jiangmen
7	Qinhuangdao	25	Taizhou	42	Yangjiang
8	Tangshan	26	Wenzhou	43	Maoming
9	Cangzhou	27	Ningde	44	Dongguan
10	Tianjin	28	Fuzhou	45	Guangzhou
11	Binzhou	29	Putian	46	Zhanjiang
12	Dongying	30	Quanzhou	47	Beihai
13	Weifang	31	Xiamen	48	Qinzhou
14	Yantai	32	Zhangzhou	49	Fangchenggang
15	Weihai	33	Chaozhou	50	Sanya
16	Qingdao	34	Shantou	51	Haikou
17	Rizhao	35	Jieyang	52	Danzhou
18	Lianyungang				

Figure 1. Schematic diagram of the study area.

3. The Construction of Disaster Response Evaluation System for Storm Surges

By making a thorough literature review of both Chinese and foreign research, and taking into account the specific conditions of coastal cities in China, this paper attempts to establish a fine-scale evaluation indicator system of disaster response capability (DRC) with a specific focus on storm surges.

3.1. Principles for Establishing an Indicator System

The establishment of a practical and scientific indicator system must follow some basic principles. Peng et al. proposed that constructing an indicator system should follow the six principles of purpose: purposefulness, completeness, operability, independence, importance, and dynamism [12]. In addition, Lu and Han proposed their own five principles: specific, measurable, achievable, realistic, and time-bound, according to principles previously applied by experts, in conjunction with disaster theory and the specific requirements of this research [13]. Meanwhile, combining the characteristics of SSDs with data gathered from the study area, four principles should be followed to establish an evaluation index system for storm surge response capacity, as proposed in this paper, including. (a) Scientific: Being scientific is the primary basis for evaluating indicator systems. SSDs can cause damage to coastal areas on a wide variety of levels, including people, property, and the environment. Therefore, it is essential that any potential indicators are chosen after a rigorous scientific screening and assessment. (b) Realistic: The aim of the evaluation model is to assess the response of cities to storm surges by identifying and analyzing any weaknesses or potential points of significant damage. Therefore, the indicators used in the system should be both easily accessible and countable, in addition to being descriptive, representative, and easy to conceptualize to ensure the ease of use of the entire system. (c) Generic: The object of evaluation for this indicator system is the city, and many coastal cities are in China. The ability to generalize indicators is among the first issues that should be addressed when establishing an indicator system. While each city has its distinctive features, there are also shared traits that must be identified to establish a standardized indicator system. Recognizing these commonalities is essential to ensure consistency and comparability across different cities. (d) Representative: This paper presents an evaluation model for disaster response capabilities related to SSDs, divided into three dimensions, each containing multiple sub-dimensions. Each sub-system should be broken down into representative indicators for individual evaluation to form a comprehensive evaluation indicator system.

3.2. Theoretical Framework for Storm Surge Response Evaluation in Coastal Cities

3.2.1. H-E-V Framework and Functional System for Disaster Systems

The primary frameworks for assessing urban flood risk are the "Probability–Consequence" model and the "Hazard–Exposure–Vulnerability (H-E-V)" model [14–16]. When comparing these two models, the "H-E-V" framework is comprehensive, clear, and practical, making it popular among scholars and research institutions. For example, the IPCC uses this framework to evaluate urban flood risks [17]. The "H-E-V" framework, commonly applied in flood risk assessments, encompasses three key components: Flood risk = Hazard (H) × Exposure (E) × Vulnerability (V).

According to Peijun Shi, the structural system of a regional disaster system (DS) comprises the disaster-incubating environment (E), disaster-causing factors (F), and disaster-bearing bodies (S), expressed as [18,19]. The system differs from Mileti's approach to structural disaster systems, where these elements are combined into a single environmental system [20]. In 2005, Peijun Shi proposed that the functional system of regional disasters

(D_f) consists of the stability of the disaster-incubating environment (S), the risk of disaster-causing factors (R), and the vulnerability of disaster-bearing bodies (V) [20]. This theory resembles Wisner's disaster system, but Wisner emphasizes the interaction between hazard factors and the affected bodies in the disaster system I have checked and revised all [21]. Peijun Shi, on the other hand, believes that hazard factors, affected bodies, and the disaster-incubating environment are equally crucial in the disaster system [18].

Based on previous studies, this research evaluates the disaster response capabilities related to storm surges from three perspectives: the stability of the disaster-incubating environment (S), the risk associated with hazard factors (R), and the vulnerability of the disaster-bearing bodies (V).

3.2.2. Theory of PPRR Model for Crisis Management

Any disaster has a life cycle that goes from inception to development, outbreak, decline, and finally to end. The crisis also has a lifecycle from its occurrence to its development, and traditional crisis management focuses more on post-disaster relief and rehabilitation, with significantly less attention paid to pre-disaster prevention and preparedness [22].

The PPRR model is a widely used theory that originates from crisis management and consists of four phases: Prevention before the crisis (Prevention), preparation before the crisis (Preparation), response during the outbreak (Response), and recovery after the crisis ends (Recovery). These four phases are the generic model of crisis management [23]. These phases correspond to the four disaster response stages, namely prevention, response, relief, and recovery, and thus define the different phases of disaster management and their associated tasks. Disaster prevention capability refers to the ability of the study areas to prevent emergencies and disasters, usually by implementing planning and countermeasures to ensure the safety of property and people. Emphasis is placed on using existing management tools as well as modern science and technology to prevent the occurrence of emergencies or disasters, primarily through the employment of disaster prevention education, increasing awareness of prevention measures, economic investment in disaster prevention, and large-scale disaster prevention projects. Disaster resilience refers to the ability of disaster-bearing bodies to resist a sudden accident or disaster and to maintain their regular function in the event of damage from a disaster. It possesses specific inherent characteristics that are primarily determined by factors such as population demographics, urban spatial organization, and socio-economic factors. The primary manifestation of disaster relief capability lies in the emergency response to disasters, which is usually determined by the government's emergency response capability, emergency resources, transportation, rescue personnel, emergency shelters, and other factors. On the other hand, the strength of a city's recovery capability is mainly influenced by insurance and economic factors [24–28].

3.3. Construction of an Evaluation Indicator System for Disaster Response Capability

Building on the theory outlined in the previous section, the assessment system for evaluating disaster response capability to SSDs comprises three components: the vulnerability of the disaster-bearing bodies, the stability of the disaster-incubating environment, and the risk of hazard factors. This study has identified suitable indicators for each component, following the principles of establishing an indicator system. In this study, the construction of the indicator system is grounded in a systematic literature review, and supported by disaster system theory. A wide range of peer-reviewed studies, policy guidelines, and technical reports in the fields of coastal vulnerability, storm surge risk assessment, and urban disaster resilience were reviewed. The following types of indicators were prioritized: (1) those widely used across multiple studies; (2) those reflecting the core dimensions of

the H-E-V and PPRR frameworks; and (3) indicator with data availability at the urban scale [5,29–57].

For example, indicators such as "population density", "length of drainage pipelines", and "proportion of elderly population" are frequently used in marine flood vulnerability assessments. "Land use ratio" is recognized as a key variable in studies on environmental stability. Although no studies were found to define "coastline type" as a specific indicator, many have highlighted its role in buffering storm surge impacts. Since this study evaluates urban disaster response from a city-level perspective, "coastline type" is considered an important component of the disaster-incubating environment. The final indicator system should ensure strong scientific validity and applicability to policy.

Regarding the vulnerability of the disaster-bearing bodies, the concept is divided into four stages based on disaster life cycle theory and the PPRR model: disaster prevention capability, disaster resistance capability, disaster relief capability, and recovery capability. In conjunction with the characteristics of the indicators and the four systemic concepts, relevant indicators have been chosen, as shown in Table 1. The stability of the disaster-incubating environment is categorized into natural and human-made environments. The natural environment encompasses various coastline types, each with different abilities to withstand storm surges. Due to varying risks of storm surge damage across different land use types, the human-made environment includes the diverse factors related to land use. The direction definition of indicators is for the subsequent analysis of indicator data using the entropy weight method. Table 2 displays the relevant indicators. Additionally, hazard factors for SSDs generally involve meteorological, hydrological, and geological elements, with the specific indicators listed in Table 3. The theoretical diagram of the evaluation system established based on the H-E-V framework and the PPRR model is displayed in Figure 2.

Table 1. Evaluation indicators for the vulnerability of disaster-bearing bodies.

Segments	Elements	Indicators	Unit	No.	Direction
Disaster prevention capability	Monitoring and early warning capability	Number of tidal stations	piece	V1	+
		Mobile phone subscribers	10,000 people	V2	+
	Education and economic input for disaster prevention	Expenditure on disaster prevention and emergency management	10,000 Yuan	V3	+
		Per capita expenditure on education	Yuan	V4	+
	Environmental factor	Coastline coefficient	km/km^2	V5	–
Disaster resistance	Demographic factors	Relative population density (within 10 km of the coastline)	People/km^2	V6	–
		Proportion of population aged 0~14	%	V7	–
		Proportion of population aged 65 and above	%	V8	–
	Spatial layout	Area of mariculture	Hectare	V9	–
	Infrastructure factors	Road mileage per unit land area	km/km^2	V10	+
		Length of drainage pipelines	km	V11	+
	Economic factors	Fishery output value	Billion Yuan	V12	–
		Proportion of the primary industry at the district (county) level including the coastline	%	V13	–
		Proportion of tourist receipts	%	V14	–
Disaster relief capability	Healthcare infrastructure	Number of hospitals per 10,000 people	pcs	V15	+
		Number of beds per 10,000 people	Bed	V16	+
		Number of doctors per 10,000 people	People	V17	+
	Transport factors	Total highway passenger traffic volume	10,000 people	V18	+
		Total highway freight traffic volume	10,000 tons	V19	+
	Economic factors	Number of shelters	pcs	V20	+

Table 1. *Cont.*

Segments	Elements	Indicators	Unit	No.	Direction
Recovery capability	Basic social security	Proportion of employees covered by basic medical insurance	%	V21	+
	Economic factors	Per capita disposable income of urban permanent residents	Yuan	V22	+
		Per capita disposable income of rural permanent residents	Yuan	V23	+
		Proportion of secondary industry	%	V24	+
		Proportion of tertiary industry	%	V25	+
		Insurance penetration	Yuan/Yuan	V26	+

Table 2. Evaluation indicators for stability of the disaster-incubating environment.

Segments	Elements	Indicators	Unit	No.
Stability of disaster-incubating environment	Coastline Stability	Percentage of estuary shoreline length	%	S1
		Percentage of bedrock shoreline length	%	S2
		Percentage of sandy shoreline length	%	S3
		Percentage of biological shoreline length	%	S4
		Percentage of muddy shoreline length	%	S5
		Percentage of the length of the reclamation and aquaculture shoreline	%	S6
		Percentage of the length of docks, artificial shorelines, and protective embankments	%	S7
	Land Stability	Percentage of farmland area	%	S8
		Percentage of forest area	%	S9
		Percentage of grassland area	%	S10
		Percentage of water area	%	S11
		Percentage of urban and rural, industrial and mining, and residential land area	%	S12
		Percentage of unutilized land area	%	S13

Table 3. Evaluation indicators for the risk of disaster-causing factors.

Segments	Elements	Indicators	Unit	No.	Direction
The risk of disaster-causing factors	Meteorological factors	Annual precipitation	mm	R1	−
		Maximum wind speed	m/s	R2	−
		Days with wind speeds exceeding 10.8 m/s	days	R3	−
	Hydrological factors	The annual average of the highest tide height	mm	R4	−
		Maximum tidal height	mm	R5	−
	Geological factors	Average altitude	m	R6	+
		Average slope	%	R7	+

The indicator framework was designed to align with the thematic priorities of the Chinese "14th Five-Year National Comprehensive Disaster Prevention and Mitigation Plan" issued by the National Disaster Reduction Commission. This includes domains such as monitoring and early-warning systems, infrastructure resilience, emergency response capacity, material reserves, technological support, and community engagement. For instance, indicators related to early-warning stations and emergency shelters directly reflect the Plan's directives on enhancing multi-source monitoring networks and shelter infrastructure. Moreover, The Sustainable Development Goals (SDGs) adopted by the United Nations in 2015 provide ideas and references for this study. The SDGs provide a unifying framework for achieving human well-being, environmental sustainability, and

disaster resilience globally by 2030. A unifying framework is provided to achieve human well-being, environmental sustainability, and disaster resilience globally by 2030. Among the 17 goals, SDG 11 (Sustainable Cities and Communities), SDG 13 (Climate Action), and SDG 1 (End Poverty) explicitly emphasize disaster preparedness, mitigation, and resilience. They integrate the main targets and priorities of the Sendai Framework for Disaster Risk Reduction [57]. Even though the SDGs are primarily intended to apply to the national level, many cities are referring to them and use the Disaster Resilience Scorecard for Cities [58] as instrument for addressing disasters. Both the SDGs and the Disaster Resilience Scorecard for Cities are intended to promote integrated and forward-looking planning, through which the resilience of cities, in terms of infrastructure, social systems, and ecological barriers, can be enhanced to achieve sustainable development.

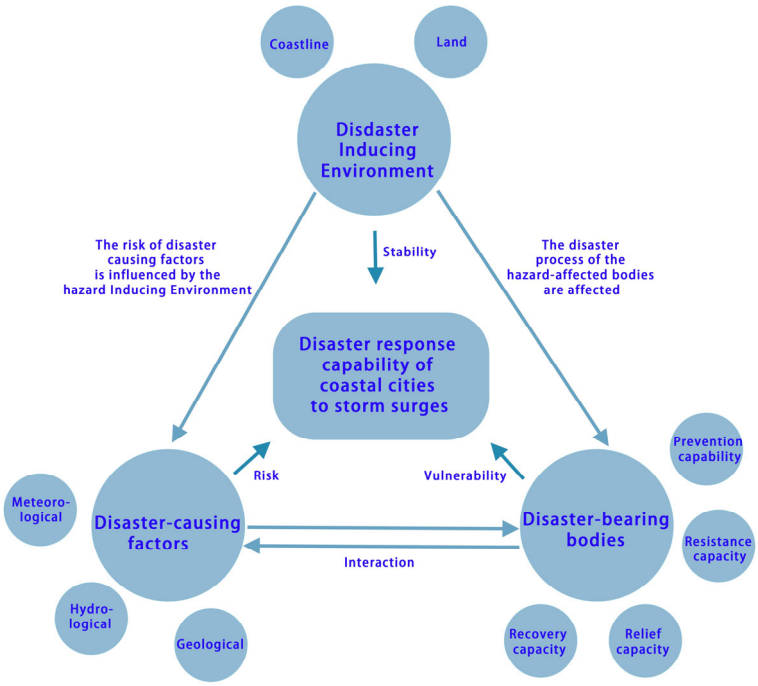

Figure 2. Theoretical map of the evaluation system.

Disaster resilience is considered to be an instrument or precondition facilitating sustainability [59]. A city's ability to effectively recover from extreme events is fundamental to achieving its long-term sustainability. Investments in early warning systems, climate-resilient infrastructure, public health services, and inclusive social protection are not only key aspects of disaster risk management, but are directly linked to the core SDG objectives of eradicating poverty, improving health, and securing livelihoods. Therefore, the systematic assessment of SSD resilience from multidimensional perspectives, including environment, infrastructure, society, and economy, is considered important for ensuring consistency between local adaptation strategies and the global sustainability agenda.

In this study, the concept of SDG objectives is fully referenced in the construction of the SSD response capacity evaluation indicator system. Specifically, indicators such as medical resources, communication access, drainage infrastructure, land use structure, income level, and insurance coverage reflect both the technical preparedness of the city and the broader socio-economic and environmental resilience advocated by the SDG framework. By using an indicator system that matches the SDGs, scientific analysis has been made more systematic and based on a stronger theory. At the same time, the policy relevance of the results has been improved. This helps support the design of more sustainable and flexible coastal management strategies for cities.

Each indicator of vulnerability of disaster-bearing bodies has been carefully selected, with its significance explained below and supported by the relevant literature [5,30,33,34,37–41,44,45,47,49–56]. Tidal detection stations provide critical real-time data for storm surge monitoring and early warning, enabling timely disaster response. A higher number of mobile users indicates a greater capacity for rapid dissemination of information during emergencies. "Mobile phone subscribers" have been regarded as an indicator for communication accessibility and the capacity for rapid information dissemination during emergencies. For instance, regions with higher mobile phone subscription rates often demonstrate better performance in early warning reception, emergency coordination, and public response [53,54]. Higher expenditures on disaster prevention and control indicate stronger institutional capacity for both pre-disaster prevention and post-disaster response. The level of education expenditure reflects public awareness and knowledge of disasters, which indirectly enhances disaster response capacity. The "Coastline Coefficient" indicator represents the abundance of marine resources in terrestrial regions. It is calculated by dividing the coastline length (in kilometers) by the land area (in square kilometers).

The high population density in vulnerable zones increases exposure and response pressure. The proportion of the population aged 0–14 and over 65 represents a group with weaker mobility and greater sensitivity to disasters. The vulnerability of aquaculture areas to storm surge inundation represents potential economic losses, and serves as a test of the resilience of marine economies. Road mileage per unit land area indicates transportation accessibility, which is vital for emergency evacuation and aid delivery. Longer drainage systems suggest better urban flood mitigation capacity. High values of fishery output suggest potential economic vulnerability in coastal areas. A high reliance on fisheries implies greater exposure to marine hazards, such as storm surges. Theoretically, this reflects sectoral dependency vulnerability and socio-ecological sensitivity. Empirical studies have confirmed that cities with higher fishery output tend to suffer more severe economic losses and face longer recovery times after coastal disasters [55,56]. The primary industry is easily affected by climate, and areas with a high proportion have weaker disaster resistance capabilities. Therefore, it is necessary to strengthen the disaster prevention system. The tourism industry is highly sensitive to the environment, and disasters will lead to a rapid decline in the tourism economy, affecting regional economic stability.

Health-related indicators, which include the number of hospitals, beds, and doctors per 10,000 persons, measure the adequacy of the emergency healthcare infrastructure. The passenger and freight transport capabilities determine the efficiency of efficient coordination and evacuation of resources and supply to disaster areas during disasters, and are important indicators of logistical support. The more shelters there are, the stronger the city's ability to accommodate disaster victims during disasters, reflecting the level of emergency reserves. The wide coverage of medical insurance can reduce the burden of post disaster medical care and improve residents' ability to recover after disasters. The per capita disposable income of urban and rural residents reflects household-level adaptive capacity and financial resilience. The secondary industry is greatly affected by infrastructure, and is prone to work stoppages after disasters, while the tertiary industry is highly dependent on the environment and has a significant impact on service interruption after disasters. Its recovery capacity needs to be evaluated. Higher penetration indicates stronger financial resilience and disaster risk transfer capacity.

Among all disaster-bearing body indicators, only population density was calculated specifically within the 10 km buffer zone from the coastline, as the population within this zone is directly exposed to storm surge impacts and plays a passive role in the disaster system, lacking the capacity to support or respond to the event. Other indicators, such as emergency transportation capacity, medical resources, disaster shelters, and institutional

mechanisms, reflect the overall DRC at the city level. These resources are not confined to the coastal zone but are spatially distributed across the urban area and can be rapidly mobilized during SSDs to support affected regions. Furthermore, although storm surges mainly affect coastal zones, the ability to respond depends on systems and resources located across the entire city behind coastal zones. Non-coastal parts of the city frequently provide logistical, economic, and administrative support during both the response and the recovery phases. Therefore, using mixed-scale data for the disaster-bearing body indicators provides a more comprehensive reflection of the overall resilience and coordination capacity of the urban system.

The spatial distribution of coastal areas and the types of shorelines are key factors influencing the resilience of coastal cities to storm surge hazards. The importance of land use and shoreline type in storm surge hazards has been noted in several studies [29,32–34,42,43,47]. Coastal land use affects the vulnerability of urban areas and their response strategies. For example, urban construction land contains dense infrastructure, which faces a higher risk of property loss and greater difficulty in evacuation during storm surge events. Agricultural land is considered highly sensitive to seawater intrusion and salinization, which may result in long-term ecological and economic damage. By contrast, areas dominated by wetlands, forests, or mangroves are regarded as natural buffers, through which wave energy is absorbed and the extent of inundation is reduced. Therefore, land use is not only seen as a reflection of regional economic functions but is considered to influence the spatial distribution of disaster resistance and exposure. In this study, the evaluation of land use stability was conducted using the primary classification from the LUCC system developed by the Chinese Academy of Sciences. At the same time, the data were clipped to a 10 km inland buffer from the coastline, following the same rationale as the population indicator, as this area is directly exposed to storm surge impacts. On the other hand, there are significant differences in the resistance of different types of shorelines to storm surge erosion and wave impacts. For instance, rocky shorelines and mangrove shorelines usually have strong natural defenses, while muddy shorelines and aquaculture shorelines are more vulnerable to erosion and overtopping. Therefore, the type of coastline is an important parameter for assessing the stability of disaster incubating environment and developing coastal management strategies.

In summary, the stability of disaster incubating environment is determined by land use and shoreline characteristics, which are regarded as essential components in the construction of an urban storm surge resilience assessment framework.

The reasons for the selection of indicators related to the disaster causal factors are listed, and these indicators are mentioned in the relevant literature [29,31,34–36,45,48].

During storm surge events, heavy rainfall is often observed, which increases coastal flood risk through surface runoff, and worsens urban waterlogging by expanding the inundation area. Therefore, annual precipitation is considered an important indicator. Maximum wind speed is regarded as a major driving factor in the formation of storm surges, as it determines the wind force on the sea surface and influences wave height, tide accumulation, and the destructive power of the hazard. Moreover, the number of days with wind speeds exceeding 10.8 m/s is used to reflect the frequency and persistence of strong wind events. Frequent occurrences are seen as an indication that coastal areas are regularly exposed to wind-driven processes, which may weaken natural defense systems and increase long-term vulnerability. The annual average of the highest tide height and maximum tidal height reflect the tidal level in the city during the year. If the annual mean maximum tide height is high, the buildup of storm surge on top of it is more likely to cause the over-topping of embankments, increasing the risk of urban inundation and infrastructure damage. Maximum tide heights are regarded as representations of the extremes reached

by astronomical tides. When they are superimposed on peak storm surges, sea levels are significantly raised, which greatly increases the intensity of the disaster. The average elevation of a city is used to determine its base height relative to sea level. Lower elevations are more susceptible to seawater inundation and flooding, and elevation is regarded as a fundamental indicator in spatial zoning of exposure and geographic sensitivity analyses. Slope is used to assess the rate of surface runoff and the retention time of standing water. Flat areas are seen as more prone to waterlogging, while steep slopes are viewed as favorable for drainage. Therefore, this indicator is considered highly important in the simulation of inundation processes and the planning of drainage systems.

Although some indicators, such as annual precipitation, are not direct causal factors of storm surges, they are still included in this study because they significantly influence disaster response conditions and tend to compound the pressure on emergency response systems during storm surge events. This study does not aim to evaluate the physical severity of storm surges themselves, but rather focuses on assessing the overall disaster response capacity of coastal cities under storm surge scenarios. Therefore, the selection of indicators prioritizes factors that are most likely to influence response effectiveness during SSDs. The inclusion of such compound risk factors reflects a more realistic urban disaster context and supports a more comprehensive resilience evaluation.

Since key data are usually updated every 5 years, most of the data in this study are based on the 2020 data for model demonstration. In this study, the most relevant indicator data for coastal cities comes from the year 2020 for analysis and evaluation. A smaller subset of data, such as those related to coastlines and land use, is taken from the period between 2020 and 2023, as these factors are likely to change slowly. Much of the data on disaster-bearing bodies were obtained from the "China City Statistical Yearbook 2021" and announcements published on the official websites of municipal governments [60]. A smaller portion of the data comes from local government responses and local news extracts obtained through a public application. Data related to disaster factors were sourced from the "Tide Table 2020" published in China and the National Oceanic and Atmospheric Administration (NOAA) of the United States, among others [61]. For the indicators "The annual average of the highest tide height" and "Maximum tidal height", the data were processed using the local mean sea level (MSL) as the vertical reference datum. During data acquisition and calculation, tide levels were adjusted relative to the MSL. The tidal reference datum for each city's observation station is explicitly documented in the "2020 Tide Table" published by Chinese authorities. Coastal data relevant to the disaster-incubating environment were extracted through the GEE platform for remote sensing image analysis, supplemented by manual identification and on-site geolocation verification (Figure 3). Land use data were sourced from the Institute of Geographic Sciences and Natural Resources Research at the Chinese Academy of Sciences and then processed using ArcGIS (Figure 4). Due to space constraints, this paper only presents the visualization of remote sensing analysis of the coastline of Weihai, Zhuhai, and Huizhou, and a visual representation of the cropped land use data for Huizhou, Zhuhai, and Weihai.

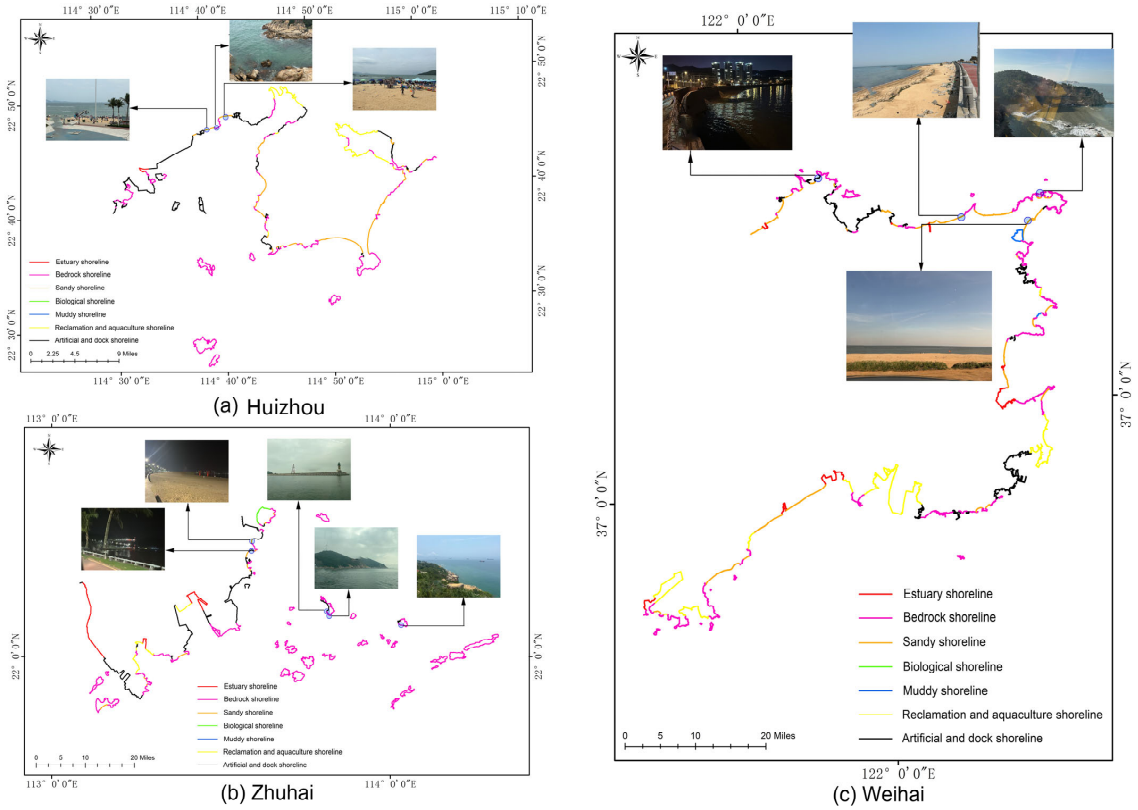

Figure 3. (**a**) Analysis of shoreline types in Huizhou and comparison with on-site research; (**b**) analysis of shoreline types in Weihai and comparison with on-site research; (**c**) analysis of shoreline types in Zhuhai and comparison with on-site research.

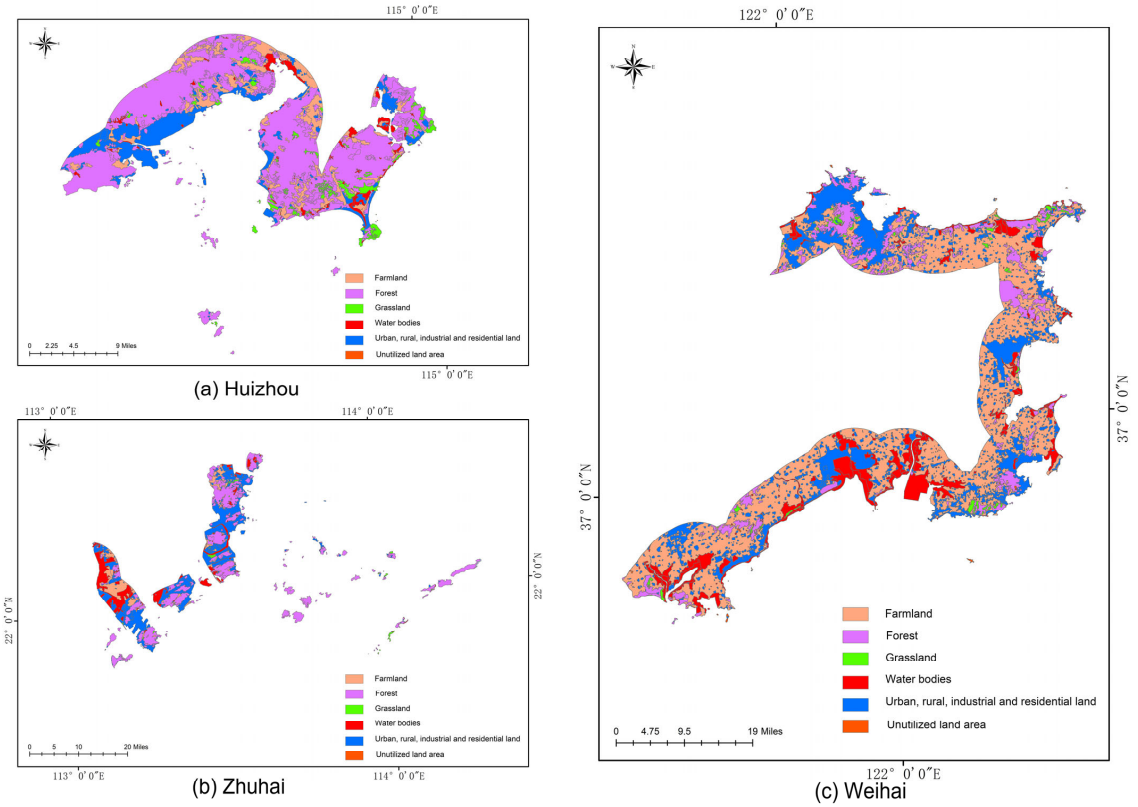

Figure 4. (**a**) Schematic diagram of coastal land use types in Huizhou; (**b**) schematic diagram of coastal land use types in Weihai; (**c**) schematic diagram of coastal land use types in Zhuhai.

4. Methods

4.1. Standardization of Original Index Data

The original data collected varied widely in terms of scale, and the scales vary greatly from one indicator to another. Therefore, it is necessary to standardize the original data before carrying out data analysis. The intention of this standardization is to group the evaluation indicators into a value between 0 and 1, and to eliminate the variability in scale between indicators and their influence on the screening indicators.

Equations (1) and (2) are the formulas used to normalize positive and negative indicators, respectively.

$$x_{ij} = \frac{v_{ij} - \max\limits_{1 \le i \le m}(v_j)}{\max\limits_{1 \le i \le m}(v_j) - \min\limits_{1 \le i \le m}(v_j)} \quad (1)$$

$$x_{ij} = \frac{\max\limits_{1 \le i \le m}(v_j) - v_{ij}}{\max\limits_{1 \le i \le m}(v_j) - \min\limits_{1 \le i \le m}(v_j)} \quad (2)$$

$\max(x_j)$ is the maximum value of all evaluation ranges in the *jth* indicator;
$\min(x_j)$ is the minimum value of all evaluation ranges in the *jth* indicator;
m is the total number of indicators (m = 30);
v_{ij} is the value of the *jth* indicator in the *ith* region;
x_{ij} is the standardized value of the indicator for the *jth* indicator in the *ith* region.

4.2. Entropy Weighted TOPSIS Method

In this study, the entropy weighted TOPSIS method was employed to analyze and evaluate the dimensions of disaster-bearing bodies and disaster-causing factors.

4.2.1. Determining Indicator Weights Using the Entropy Weight Method

(a) After data preprocessing, calculate the proportion "p_{ij}" of index value of project i under index j: "p_{ij}" is calculated as in Equation (3):

$$p_{ij} = \frac{x_{ij}}{\sqrt{\sum\limits_{i=1}^{n} x_{ij}}} \quad (3)$$

p_{ij} is the proportion of the *ith* sample value under the *jth* indicator.

(b) Calculate the entropy of each indicator, the formula is shown in Equation (4):

$$e_j = -k\sum_{i=1}^{n} p_{ij} In(p_{ij}) \quad (4)$$

for which $k = 1/\ln(n) > 0$, and $e_j \ge 0$.

e_j is the information entropy of the *jth* indicator.

(c) Define the degree of difference for the *jth* indicator as follows:

$$d_j = 1 - e_j \quad (5)$$

(d) Calculate the entropy weight, which is calculated as in Equation (5):

$$w_j = \frac{d_j}{\sum\limits_{j=1}^{m} d_j} \quad (6)$$

w_j is the weight of the *jth* indicator.

The greater the weight, the more information the indicator reflects, and the more important the indicator is in the comprehensive evaluation.

4.2.2. Using TOPSIS Method to Determine Comprehensive Scores

(a) Build the standardized matrix of weight: Calculate the standardized value "z_{ij}" of weight and build the standardized matrix of weight. The formula is shown in Equation (6):

$$z_{ij} = w_j x_{ij} \tag{7}$$

(b) Determine the ideal solution and the anti-ideal solution, the formulas are shown in Equations (7) and (8):

$$z_j^+ = \{\max Z_{ij}\} \tag{8}$$

$$z_j^- = \{\min Z_{ij}\} \tag{9}$$

Z_i^+ is the ideal solution;
Z_i^- is the anti-ideal solution.

(c) Calculate distance scale: Distance scale calculated by Euclidean distance is the distance between each objective and the ideal solution or the anti-ideal solution. The calculation formulas are shown in Equations (9) and (10).

$$D_i^+ = \sqrt{\sum_{j=1}^{m} (Z_{ij} - Z_j^+)^2} \tag{10}$$

$$D_i^- = \sqrt{\sum_{j=1}^{m} (Z_{ij} - Z_j^-)^2} \tag{11}$$

D_i^+ is the distance between the objective and the ideal solution Z^+;
D_i^- is the distance between the objective and the anti-ideal solution Z^-.

(d) Calculate the closeness degree of the ideal solution. The calculation formula is shown in Equation (11):

$$C_i = \frac{D_i^-}{D_i^- + D_i^+} \tag{12}$$

Evaluation subjects are ranked based on the size of the C_i value, and proximity is used to determine the composite score and to provide the evaluation results. In this study, the entropy-weighted TOPSIS method is employed to assess the vulnerability of the disaster-bearing body and the risk of disaster-causing factors. The higher the value of C_i, the better the result. Therefore, according to the definition, the higher the C_i value, the lower the vulnerability of the disaster-bearing body, and the lower the risk of disaster-causing factors.

4.3. Weight Rank Sum Ratio (WRSR)

The rank sum ratio (RSR) is a commonly used evaluation model. It differs from other evaluation models in that it incorporates secondary correction during the calculation process, resulting in improved reliability in its practical applications. In the comprehensive evaluation, the value of the rank sum ratio can contain information about all evaluation indicators, and a larger RSR value indicates a better evaluation result. The advantages of this evaluation method are mainly that it is insensitive to outliers and that it can be graded for evaluation objects. The WRSR method was employed to analyze the stability

of the disaster-incubating environment. The calculation steps and formulas are shown in Equations (12)–(14).

$$RSR_i = \frac{1}{mn}\sum_{j=1}^{m} R_{ij} \tag{13}$$

$$WRSR_i = \frac{1}{n}\sum_{j=1}^{m} w_j R_{ij} \tag{14}$$

$$\sum_{j=1}^{m} w_j = 1 \tag{15}$$

$i = 1, 2, \cdots, n$

$j = 1, 2, \cdots, m$

n is the number of evaluated objects

m is the number of indicators

R_{ij} is the rank of the ith row and jth column elements

w_j is the weight of the jth evaluation indicator

The rank of each indicator becomes particularly important when weighting the results of the RSR. According to the "Guideline for risk assessment and zoning of SSD", the evaluation method for the stability of SSDs is divided into four levels of land use stability based on SSDs, with four levels being the highest stability (rank = 4), as shown in Table 4 [62]. Meanwhile, according to Gornitz and Hammar-Klose and Thierer, the stability of natural environment coastlines is divided into five levels, ranging from very low stability (rank = 1) to very high stability (rank = 5), as shown in Table 5 [63,64]. In this study, the disaster-incubating environment indicator weights will be determined based on their ranks.

Table 4. Stability levels of different land use types.

Land Use Type	Stability Level
Farmland	1
Woodland	1
Grassland	1
Water bodies	1
Urban, rural, industrial, and residential land	4
Unutilized land area	1

Table 5. Stability levels of different shoreline types.

Shoreline Type	Stability Level
Estuary shoreline	3
Bedrock shoreline	5
Sandy shoreline	2
Biological shoreline	4
Muddy shoreline	2
The reclamation and aquaculture shoreline	2
The docks, artificial shorelines, and protective embankments	4

The two methods were not combined arbitrarily but selected based on the characteristics of the indicator datasets. The entropy weighted TOPSIS method was applied to the dimensions of disaster-bearing bodies and disaster-causing factors because their associated indicators are numerical and heterogeneous. The weight of indicators needs to be obtained through the entropy weight method, and then the ranking results can be obtained through TOPSIS. By contrast, for the disaster-incubating environment dimension, indicators were

based on the length of different shoreline types and the area of different land use categories. The weights of these indicators are obtained through the authoritative stability scores in the existing literature, which are not suitable for obtaining using the entropy weight method. Furthermore, shoreline and land use types vary significantly across cities, and the evaluation in this dimension emphasizes spatial composition rather than numerical magnitude. Therefore, a more suitable WRSR method was adopted, and ideal-type cities serve as benchmarks to evaluate relative stability across coastal cities.

5. Results

Firstly, the stability of the disaster-incubating environment (S), the risk of disaster-causing factors (R), and the vulnerability of the disaster-bearing bodies (V) are analyzed, and the results are obtained separately. Subsequently, employing the H-E-V framework commonly utilized in flood risk assessments, the formula Flood Risk = Hazard (H) × Exposure (E) × Vulnerability (V) is adapted to compute the capability for responding to SSDs. To facilitate the analysis and observation, the analytical results concerning the disaster-incubating environment, the disaster-bearing body, and the disaster-causing factor were multiplied by 10, respectively. This adjustment facilitates the generation and interpretation shown in Figure 5, which visually depicts the computed disaster response capability. Moreover, the weights of the indicators obtained through the entropy weighting method are displayed in Table 6, and the scores of the evaluation of the response capability to SSDs in coastal cities of China are shown in Table 7. The visualization maps of vulnerability of disaster-bearing bodies, risk of disaster-causing factors, and stability of disaster-prone environments levels based on storm surges are displayed in Figures 6a, 6b and 6c, respectively. The visualization map of storm surge response capability levels for coastal cities in China is displayed in Figure 6d.

Table 6. Entropy-Based Weights of Disaster Response Capability Indicators.

Indicators of the Vulnerability of Disaster-Bearing Bodies.	Weights	Indicators of the Risk of Disaster-Causing Factors	Weights
Number of tidal stations	5.42%	Annual precipitation	0.9789
Mobile phone subscribers	6.38%	Maximum wind speed	0.9912
Expenditure on disaster prevention and emergency management	9.63%	Days with wind speeds exceeding 10.8 m/s	0.9934
Per capita expenditure on education	3.54%	The annual average of the highest tide height	0.9780
Coastline coefficient	1.56%	Maximum tidal height	0.9717
Relative population density (within 10 km of the coastline)	13.10%	Average altitude	0.8942
Proportion of population aged 0~14	3.38%	Average slope	0.9382
Proportion of population aged 65 and above	2.00%		
Area of mariculture	2.95%		
Road mileage per unit land area	8.17%		
Length of drainage pipelines	4.74%		
Fishery output value	11.75%		
Proportion of the primary industry at the district (county) level including the coastline	6.42%		
Proportion of tourist receipts	3.18%		
Number of hospitals per 10,000 people	5.67%		
Number of beds per 10,000 people	1.29%		
Number of doctors per 10,000 people	2.15%		
Total highway passenger traffic volume	1.20%		
Total highway freight traffic volume	0.31%		
Number of shelters	0.46%		

Table 6. *Cont.*

Indicators of the Vulnerability of Disaster-Bearing Bodies.	Weights	Indicators of the Risk of Disaster-Causing Factors	Weights
Proportion of employees covered by basic medical insurance	1.54%		
Per capita disposable income of urban permanent residents	1.64%		
Per capita disposable income of rural permanent residents	0.40%		
Proportion of secondary industry	1.66%		
Proportion of tertiary industry	0.83%		
Insurance penetration	0.65%		

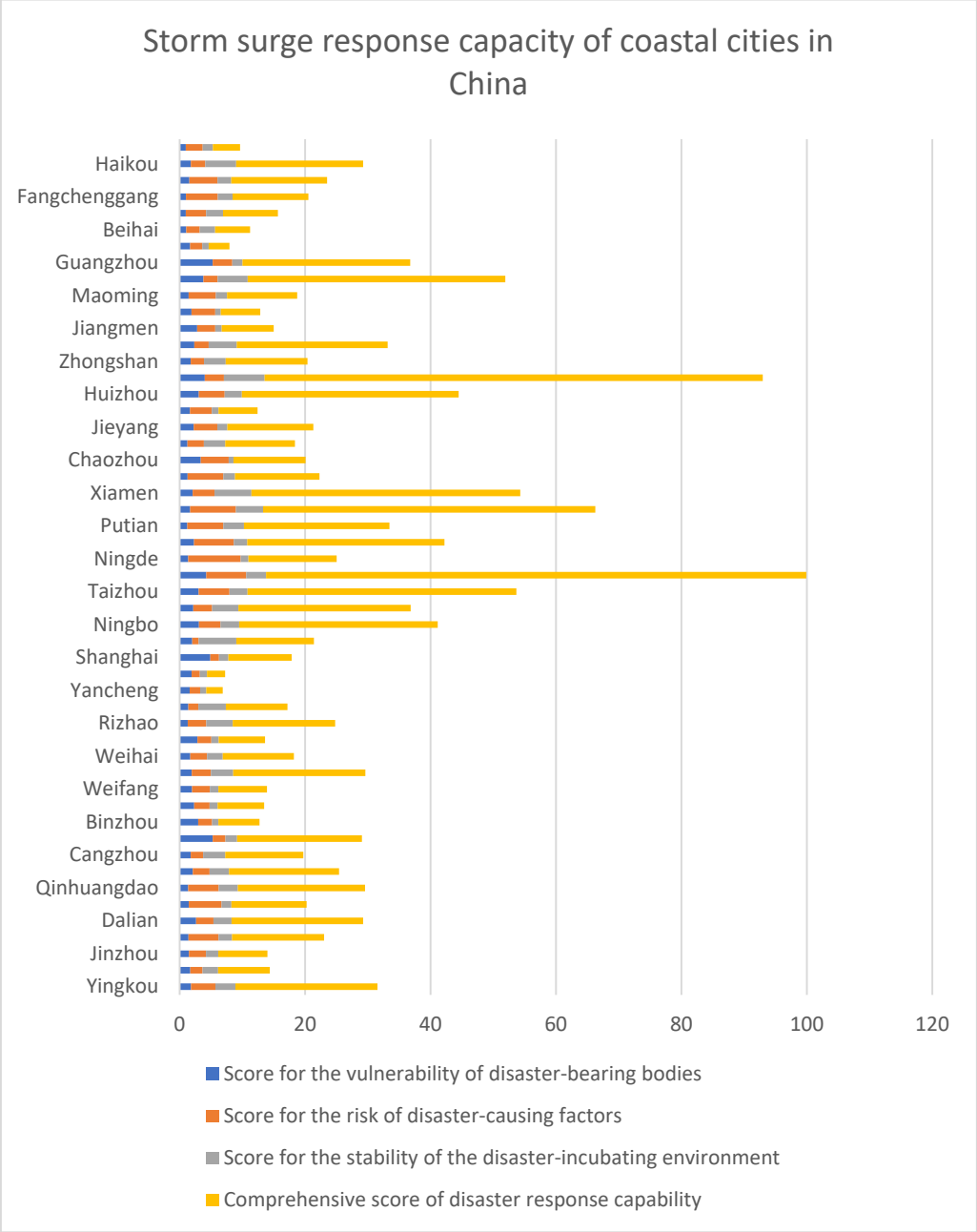

Figure 5. Storm surge response capabilities of coastal cities in China.

Table 7. Score of the response capability evaluation to SSDs in Chinese coastal cities.

City	Vulnerability Scores for Disaster-Bearing Bodies	Score for the Risk of Disaster-Causing Factors	Score for Stability of Disaster-Incubating Environment	Comprehensive Score of DRC
Yingkou	1.83	3.87	3.20	22.64
Panjin	1.71	1.96	2.46	8.24
Jinzhou	1.48	2.72	1.95	7.86
Huludao	1.43	4.77	2.15	14.68
Dalian	2.64	2.77	2.87	20.97
Dandong	1.46	5.23	1.57	11.98
Qinhuangdao	1.37	4.87	3.04	20.28
Tangshan	2.12	2.65	3.12	17.52
Cangzhou	1.78	1.98	3.53	12.44
Tianjin	5.28	2.03	1.86	19.91
Binzhou	2.97	2.21	1.00	6.57
Dongying	2.33	2.45	1.30	7.40
Weifang	1.98	2.84	1.38	7.74
Yantai	1.95	3.05	3.54	21.07
Weihai	1.7	2.68	2.49	11.35
Qingdao	2.84	2.23	1.17	7.39
Rizhao	1.31	2.95	4.22	16.32
Lianyungang	1.4	1.6	4.38	9.82
Yancheng	1.62	1.66	0.97	2.62
Nantong	1.91	1.32	1.15	2.89
Shanghai	4.91	1.37	1.50	10.10
Jiaxing	2.02	1.02	6.01	12.38
Ningbo	3.08	3.45	2.98	31.64
Zhoushan	2.18	3.01	4.19	27.47
Taizhou	3.03	4.92	2.88	42.86
Wenzhou	4.26	6.35	3.18	86.13
Ningde	1.36	8.38	1.23	14.07
Fuzhou	2.31	6.33	2.15	31.44
Putian	1.23	5.74	3.29	23.20
Quanzhou	1.67	7.3	4.34	52.96
Xiamen	2.09	3.48	5.89	42.86
Zhangzhou	1.28	5.69	1.85	13.48
Chaozhou	3.37	4.47	0.76	11.49
Shantou	1.24	2.63	3.41	11.12
Jieyang	2.26	3.75	1.61	13.69
Shanwei	1.65	3.48	1.08	6.22
Huizhou	3.06	4.12	2.74	34.57
Shenzhen	4.01	3.05	6.49	79.41
Zhongshan	1.78	2.12	3.45	13.03
Zhuhai	2.36	2.27	4.49	24.05
Jiangmen	2.79	2.9	1.02	8.29
Yangjiang	1.89	3.8	0.88	6.29
Maoming	1.44	4.35	1.78	11.17
Dongguan	3.81	2.25	4.79	41.07
Guangzhou	5.27	3.14	1.62	26.73
Zhanjiang	1.67	1.94	1.02	3.31
Beihai	1.06	2.15	2.45	5.58
Qinzhou	1	3.23	2.71	8.74
Fangchenggang	1.01	5.09	2.35	12.08
Sanya	1.56	4.48	2.19	15.29
Haikou	1.8	2.28	4.93	20.25
Danzhou	1	2.69	1.61	4.34

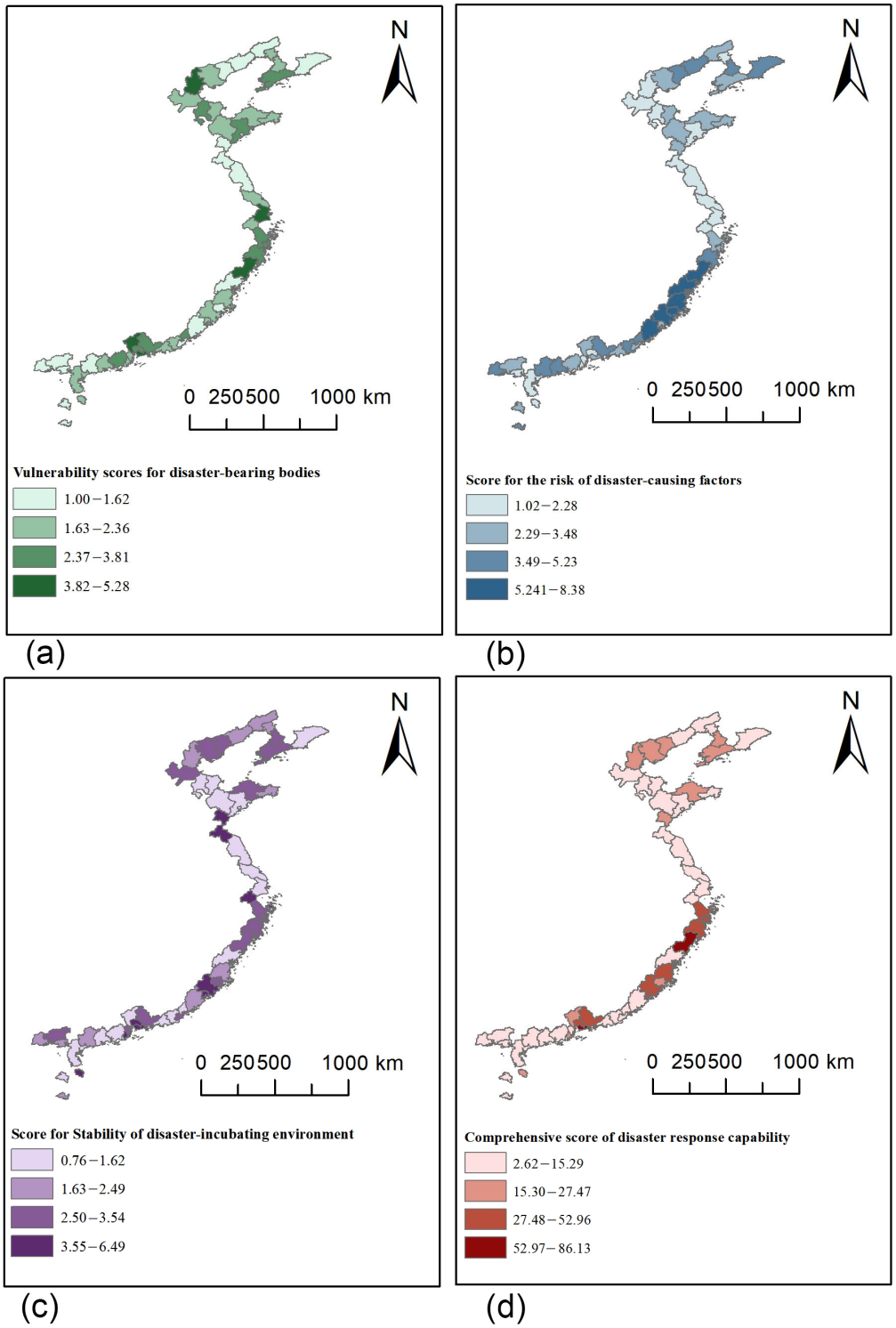

Figure 6. (**a**) Thermal map of vulnerability score of disaster bearing body; (**b**) thermal map of risk score of disaster causing factors; (**c**) thermal map of stability score of disaster- incubating environment; (**d**) thermal map of comprehensive score for DRC.

6. Discussion

6.1. Interpretation of Results

The present analysis focuses on the evaluation of SSD risk and response capabilities across various cities. Scores for the vulnerability of disaster-bearing bodies, the risk of disaster-causing factors, the stability of the disaster-incubating environment, and the overall DRC were obtained. By examining the comprehensive DRC scores for 52 Chinese coastal

cities, the various strengths and weaknesses of the DRC of different coastal cities can be more easily identified, which is of great significance for SSD preparedness planning in coastal cities.

According to the study results, Chaozhou scored the lowest in assessing the stability of the disaster-incubating environment, with a score of 0.76. By contrast, Shenzhen scored the highest in the same assessment, scoring 6.49. Shenzhen is a highly urbanized and economically developed prefecture-level city whose coastline consists mainly of rocky and artificial shorelines. Shanghai, an economically developed city, does not have a very high disaster-incubating environmental stability score because a portion of its coastal area is used for agricultural development. Lower scores in this category suggest an environment prone to conditions that can foster disasters, such as unstable geological conditions. For these cities, effective urban planning and environmental management are critical. Storm surge defense strategies for these cities should concentrate on coastal and land use planning while also increasing the resilience of the disaster-bearing bodies to minimize vulnerability. Strategies should include sustainable land use practices, regular environmental assessments, and proactive measures to address and to mitigate potential environmental hazards. Cities with higher scores, indicating a stable environment, should stay active. Continued efforts in environmental monitoring and sustainable practices are essential to maintain stability and to prevent the incubation of disaster-prone conditions.

Based on the scores in the vulnerability component, it is understood that Qinzhou and Danzhou tied for the lowest score of 1, while Guangzhou had the highest score of 5.27. Tianjin, Guangzhou, Shanghai, Wenzhou, and Shenzhen ranked in the top five scores, indicating that these five cities have low vulnerability. Putian, Beihai, Fangchenggang, Qinzhou, and Danzhou are highly vulnerable. This variation indicates a pronounced disparity in how different cities are equipped to handle disasters. Cities with lower scores in this category will likely face more significant challenges due to weaker infrastructure, higher population densities, or insufficient preparedness measures. These cities must prioritize enhancing their resilience through targeted investments in infrastructure fortification, stringent building codes, and comprehensive disaster preparedness programs.

Conversely, cities with higher scores demonstrate a higher degree of resilience. Although better prepared, these cities should continue to innovate and strengthen their existing measures to maintain and improve their preparedness levels. Cities with low vulnerability to hazards are economically developed, while cities with high vulnerability are those with smaller economies and populations along China's coasts. The degree of vulnerability of the disaster-bearers is reflected in the link between the degree of development of the cities. Indeed, the reality is that developed cities are more resilient to disasters.

The risk of disaster-causing factors also shows considerable variation, with scores ranging from 1.02 to 8.38. This wide range underscores the differing levels of exposure to natural or artificial hazards in the cities. Jiaxing has the lowest score of 1.02, while Ningde has the highest score of 8.38. Ningde, Qinzhou, Wenzhou, Fuzhou, and Putian had the top five scores, indicating that their riskiness of disaster-causing factors was low. Meanwhile, according to the results, Yancheng, Lianyungang, Shanghai, Nantong, and Jiaxing have a higher risk of disaster-causing factors. High-risk cities are likely to be more prone to events such as geological instability, extreme weather conditions, or industrial accidents. For these cities, the focus should be on enhancing early warning systems, implementing robust risk mitigation strategies, and maintaining continuous monitoring of potential hazards. On the other hand, cities with lower risk scores must maintain their current safety measures while staying vigilant to new or evolving threats that could impact their risk profiles.

The comprehensive DRC score ranges from 2.62 to 86.12. Yancheng received the lowest score, and Wenzhou received the highest score. The top five cities were Wenzhou, Shenzhen,

Quanzhou, Taizhou, and Xiamen, while the bottom five were Shanwei, Beihai, Danzhou, Zhanjiang, Nantong, and Yancheng. Notably, Shanghai scored only 10.09, indicating that developed cities do not necessarily possess more excellent capability to withstand storm surges. A high composite score in environment and climate for coastal cities complements the city's disaster resilience conditions. For example, Shanghai is a developed city. The geographical location, climatic conditions, natural environment, and urban layout are not conducive to resisting storm surges. Although Shanghai has a well-developed disaster prevention infrastructure and adequate staffing and funding for commissioners, the economic losses will be more severe than in other cities.

In summary, analyzing the maximum and minimum values across the four categories provides critical insights into the disaster preparedness and response capabilities of different cities. The disparities highlighted in the vulnerability, risk, environmental stability, and response capability underscore the need for tailored strategies to address the specific challenges faced by each city. For cities with high vulnerability and risk scores, prioritizing resilience and mitigation measures is essential. By contrast, cities with stable environments and robust response capabilities should focus on maintaining and enhancing their existing measures. This comprehensive approach ensures that all cities, regardless of their current scores, are better prepared to handle future disasters and to protect their populations effectively.

6.2. Uncertainty Analysis

While the model demonstrates significant potential in its current form, and the multi-indicator integrated assessment method combining entropy weighted TOPSIS and WRSR was adopted, it also has uncertainties that warrant discussion and refinement in future applications.

Firstly, a primary limitation of the evaluation results is its reliance on data from the year 2020. This temporal constraint may limit the model's ability to capture changes. The reason for using the 2023 remote sensing data is that field surveys were conducted in the same year, making it the most accurate and consistent choice for shoreline classification. Consequently, the results derived from the 2020 dataset might not fully reflect the present-day status or emerging trends in coastal city resilience. This temporal mismatch highlights the need for regular updates to the underlying data to ensure that the model remains reflective of contemporary realities. Although this temporal mismatch may limit the model's ability to fully reflect real-time conditions or recent developments in coastal resilience, the analytical framework itself remains valid and adaptable. As more consistent and updated datasets become available, the model can be recalibrated accordingly. This flexibility allows for its continued application in monitoring and assessing storm surge response capacity over time.

Secondly, although the entropy weighting method was used to improve objectivity, the selection and weighting of indicators still involve subjectivity. The entropy method focuses on the variability of data but may not fully reflect the actual importance in disaster response. The WRSR method helps reduce the effect of extreme values, but its ranking of environmental stability is based on empirical classification, which may oversimplify complex natural processes. In addition, the method assumes that indicators are independent. In reality, urban density, infrastructure, and economic power are often closely related. This may lead to redundancy and affect the accurate assessment of the vulnerability of the disaster-bearing body.

Finally, the current models are based on cross-sectional analysis and do not reflect changes in storm surge risk and disaster response capacity over time. As climate trends, urban development, and governance continue to change, the results of this study should be seen as a static assessment at a given time rather than a precise forecast of future conditions.

Despite this limitation, the model is inherently designed with flexibility to integrate updated datasets as they become available. This design feature enables the model to remain dynamic and adaptable, allowing for the ongoing evaluation of coastal cities' resilience under changing conditions. Such updates would also provide opportunities for longitudinal analyses to track resilience improvements or deteriorations over time. Methodologically, the model employs a robust framework that facilitates seamless incorporation of new datasets without requiring substantial modifications to its structure. By recalibrating input parameters based on updated information, the model can maintain its validity and reliability in assessing resilience across different time periods. This capability underscores its potential to support evidence-based policymaking and adaptive planning in coastal cities.

In conclusion, although there are current challenges of data temporality, methodological subjectivity, and dynamic adaptation, the storm surge resilience evaluation model's design allows for iterative improvements through data updates. This adaptability ensures its long-term utility in evaluating and enhancing the resilience of coastal cities, thereby supporting sustainable urban development and disaster risk reduction efforts.

7. Conclusions

From the perspective of the disaster response capability related to SSDs, this paper constructed an evaluation indicator system for the storm surge response capacities of 52 coastal cities in China through the H-E-V framework, a functional system for disaster systems, and PPRR theory. The system used in this study consists of three dimensions, which are stability of the disaster-incubating environment (S), the risk of disaster-causing factors (R), and the vulnerability of the disaster-bearing bodies (V). Meanwhile, through government surveys and consultation of statistical yearbooks, a comprehensive evaluation of these cities was conducted using the entropy weighted TOPSIS method and weight rank sum ratio, ultimately producing scores that display their respective SSD response capability levels.

This study has filled a gap in the research on the urban level of DRC and has discussed many aspects of the SSD resilience among coastal cities. In the evaluation of the disaster response capabilities of storm surge, Tianjin, Ningde, and Shenzhen demonstrated strong performance across three critical dimensions: the vulnerability of disaster-bearing entities, the risk associated with disaster-causing factors, and the stability of environments prone to disaster incubation. Each city showed significant strengths in mitigating potential threats and maintaining stability in the face of potential hazards. Conversely, Dandong, which shares the same ranking as Qinzhou, Jiaxing, and Chaozhou, exhibited weaker performance in these crucial areas. These cities faced challenges in minimizing vulnerabilities, managing disaster risks, and ensuring environmental stability, which may necessitate targeted interventions to enhance their disaster resilience. Moreover, Yancheng has the weakest storm surge response capability, while Wenzhou has the strongest. The results not only enable coastal cities to compare and learn from each other more easily, from each other's strengths and weaknesses when it comes to disaster response, but they provide a reference and basis for improving the disaster response capacities and planning mechanisms of coastal cities.

Author Contributions: All authors contributed to the study conception and design. Material preparation, data collection, and analysis were performed by S.C. and L.Z. The first draft of the manuscript was written by S.C., and all authors commented on previous versions of the manuscript. All authors have read and agreed to the published version of the manuscript.

Funding: The authors declare that this study received funding from "Research and Application of Key Technologies for Campus Zero Carbonization Transformation of New Energy Systems" (Project number is 6122020002 and Contract number is Z612302004) by China Yangtze Power Co., Ltd. (CYPC)

and Three Gorges Electric Energy Co., Ltd. The funder was not involved in the study design, collection, analysis, interpretation of data, the writing of this article or the decision to submit it for publication.

Data Availability Statement: The raw data supporting the conclusions of this article will be made available by the authors on request.

Acknowledgments: The authors are grateful for the data support provided by the APSEC Center of Tianjin University. At the same time, the financial support for the "Research and Application of Key Technologies for Campus Zero Carbonization Transformation of New Energy Systems" project is appreciated.

Conflicts of Interest: The authors have no relevant financial or non-financial interests to disclose.

References

1. Xin, L.; Yinyin, W. Study on disaster of storm surges and prevention measures in China. In Proceedings of the 2010 2nd IEEE International Conference on Information and Financial Engineering, Chongqing, China, 17–19 September 2010; IEEE: Piscataway, NJ, USA, 2010. [CrossRef]
2. Lin, J.; Xu, Y.; Hou, Y.; Xue, X. Spatio-temporal distribution, composition and influencing factors of economic losses from storm surge disasters: An empirical study from China (2007–2016). *Int. J. Disaster Risk Reduct.* **2023**, *90*, 103669. [CrossRef]
3. Shi, X.; Zhang, Y.; Liu, S.; Yang, L.; Yu, L.; Zhang, Y.; Jia, N.; Tian, Z. Mapping Storm Surge Risk at County Level in Coastal Areas of China. *J. Mar. Sci. Eng.* **2025**, *13*, 427. [CrossRef]
4. Tan, Y.; Zhang, W.; Feng, X.; Guo, Y.; Hoitink, A.J.F. Storm surge variability and prediction from ENSO and tropical cyclones. *Environ. Res. Lett.* **2023**, *18*, 024016. [CrossRef]
5. Meng, D.; Liu, Y.; Wang, Z.; Yang, X.; Liu, X.; Zhang, J.; Gao, K. Decreasing Vulnerability of Storm Surge Disasters in Coastal Cities of China over the Past 30 Years. *J. Mar. Sci. Eng.* **2023**, *11*, 128. [CrossRef]
6. Yi, X.; Sheng, K.; Wang, Y.; Wang, S. Can economic development alleviate storm surge disaster losses in coastal areas of China? *Mar. Policy* **2021**, *129*, 104531. [CrossRef]
7. Xianwu, S.; Jufei, Q.; Bingrui, C.; Xiaojie, Z.; Haoshuang, G.; Jun, W.; Zhuyuan, B. Storm surge risk assessment method for a coastal county in China: Case study of Jinshan District, Shanghai. *Stoch. Environ. Res. Risk Assess.* **2020**, *34*, 627–640. [CrossRef]
8. Huang, X.; Jin, H.; Bai, H. Vulnerability assessment of China's coastal cities based on DEA cross-efficiency model. *Int. J. Disaster Risk Reduct.* **2019**, *36*, 101091. [CrossRef]
9. Blankespoor, B.; Dasgupta, S.; Lange, G.-M. Mangroves as a protection from storm surges in a changing climate. *Ambio* **2016**, *46*, 478–491. [CrossRef] [PubMed]
10. Nguyen, X.H.; Nguyen, X.T.; Nguyen, H.H.; Tran, T.T.; Le, D.Q. Assessment of storm surge risk in aquaculture in the Northern coastal area of Vietnam. *Vietnam. J. Sci. Technol. Eng.* **2018**, *60*, 89–94. [CrossRef]
11. Xu, H.; Xu, K.; Bin, L.; Lian, J.; Ma, C. Joint Risk of Rainfall and Storm Surges during Typhoons in a Coastal City of Haidian Island, China. *Int. J. Environ. Res. Public Health* **2018**, *15*, 1377. [CrossRef]
12. Peng, Z.; Zhang, A.; Bingrui, S.; Wang, Z.; Bai, Y. Design Principles and Construction Process of a Comprehensive Evaluation Index System. *Sci. Res. Manag.* **2020**, *38*, 209–215. (In Chinese)
13. Lu, X.; Han, Z. Emergency management in China: Towards a comprehensive model? *J. Risk Res.* **2018**, *22*, 1425–1442. [CrossRef]
14. Meyer, V.; Scheuer, S.; Haase, D. A multicriteria approach for flood risk mapping exemplified at the Mulde river, Germany. *Nat. Hazards* **2009**, *48*, 17–39. [CrossRef]
15. Haynes, H.; Haynes, R.; Pender, G. Integrating socio-economic analysis into decision-support methodology for flood risk management at the development scale (Scotland). *Water Environ. J.* **2008**, *22*, 117–124. [CrossRef]
16. Giupponi, C.; Mojtahed, V.; Gain, A.K.; Biscaro, C.; Balbi, S. Integrated Risk Assessment of Water-Related Disasters. In *Hydro-Meteorological Hazards, Risks and Disasters*; Elsevier: Amsterdam, The Netherlands; pp. 163–200. [CrossRef]
17. Pachauri, R.; Meyer, L.; Hallegatte, S.; Hegerl, G.; Van Ypersele, J.P.; Brinkman, S. Climate Change 2014 Synthesis Report [Internet]. IPCC. Gian-Kasper Plattner. 2014. Available online: https://www.ipcc.ch/site/assets/uploads/2018/02/SYR_AR5_FINAL_full.pdf (accessed on 29 June 2025).
18. Shi, P. On the Theory and Practice of Disaster Research. *J. Nanjing Univ.* **1991**, *11*, 37–42. (In Chinese)
19. Shi, P. Theory and Practice on Disaster System Research in a Fourth Time. *J. Nat. Disasters* **2005**, *06*, 1–7. (In Chinese)
20. Mileti, D. *Disasters by Design a Reassessment of Natural Hazards in the United States*; J.H. Press: Washington, DC, USA, 1999. [CrossRef]
21. Wisner, B.; Blaikie, P.; Cannon, T.; Davis, I. *At Risk: Natural Hazards, People's Vulnerability and Disasters*, 2nd ed.; Routledge: London, UK, 2004.

22. De Smet, H.; Schreurs, B.; Leysen, J. The Response Phase of the Disaster Management Life Cycle Revisited Within the Context of "Disasters Out of the Box. *J. Homel. Secur. Emerg. Manag.* **2015**, *12*, 319–350. [CrossRef]
23. Anand, A.; Buhagiar, K.; Kozachenko, E.; Parameswar, N. Exploring the role of knowledge management in contexts of crisis: A synthesis and way forward. *Int. J. Organ. Anal.* **2022**, *31*, 2953–2978. [CrossRef]
24. Li, X. Study on Assessment of Urban Composite Disaster-Bearing Capacity. *J. Xi'an Univ. Archit. Technol.* **2012**, *4*, 489–494. (In Chinese)
25. Wang, J.; Gong, Q.; Yu, Y.; Yuan, S.; Chen, J.; Huang, G. Evaluation of Comprehensive Disaster-Bearing Capacity of Urban Natural Disasters in the Guangdong-Hong Kong-Macao Greater Bay Area. *Geogr. Res.* **2020**, *39*, 2189–2199. (In Chinese)
26. Zerger, A.; Smith, D.I.; Hunter, G.J.; Jones, S.D. Riding the storm: A comparison of uncertainty modelling techniques for storm surge risk management. *Appl. Geogr.* **2002**, *22*, 307–330. [CrossRef]
27. Torres-Vera, M.A.; Antonio Canas, J. A lifeline vulnerability study in Barcelona, Spain. *Reliab. Eng. Syst. Saf.* **2003**, *80*, 205–210. [CrossRef]
28. Zhang, M.; Liu, Y.; Yuan, Y. Research on the Assessment of Urban Comprehensive Disaster-Bearing Capacity Based on Variable Fuzzy Clustering. *J. Catastrophology* **2012**, *27*, 135–138. (In Chinese)
29. Mahamoud, A.; Gzam, M.; Mohamed, N.A.; Soulé, H.H.; Montacer, M. A preliminary assessment of coastal vulnerability for Ngazidja Island, Comoros Archipelago, Western Indian Ocean. *Environ. Earth Sci.* **2022**, *81*, 44. [CrossRef]
30. Bormann, H.; Kebschull, J.; Gaslikova, L.; Weisse, R. Model-based assessment of climate change impact on inland flood risk at the German North Sea coast caused by compounding storm tide and precipitation events. *Nat. Hazards Earth Syst. Sci.* **2024**, *24*, 2559–2576. [CrossRef]
31. Qian, X.; Hwang, S.; Son, S. A Study on Key Determinants in Enhancing Storm Surges Along the Coast: Interplay Between Tropical Cyclone Motion and Coastal Geometry. *J. Geophys. Research. Ocean.* **2024**, *129*, e2023JC020400. [CrossRef]
32. Chen, B.; He, J.; He, Z.; Li, L.; Chen, Q.; Li, F.; Chu, D.; Cao, Z.; Yang, X. Potential impacts of storm surge-induced flooding based on refined exposure estimation: A case study in Zhoushan island, China. *Geomat. Nat. Hazards Risk* **2023**, *14*, 2232080. [CrossRef]
33. Liu, X.; Liu, Y.; Wang, Z.; Yang, X.; Zeng, X.; Meng, D. Comprehensive Assessment of Vulnerability to Storm Surges in Coastal China: Towards a Prefecture-Level Cities Perspective. *Remote Sens.* **2023**, *15*, 4828. [CrossRef]
34. Islam, M.F.; Bhattacharya, B.; Popescu, I. Flood risk assessment due to cyclone-induced dike breaching in coastal areas of Bangladesh. *Nat. Hazards Earth Syst. Sci.* **2019**, *19*, 353–368. [CrossRef]
35. Liu, Y.; Lu, C.; Yang, X.; Wang, Z.; Liu, B. Fine-Scale Coastal Storm Surge Disaster Vulnerability and Risk Assessment Model: A Case Study of Laizhou Bay, China. *Remote Sens.* **2020**, *12*, 1301. [CrossRef]
36. Mohanty, M.P.; Sherly, M.A.; Ghosh, S.; Karmakar, S. Tide-rainfall flood quotient: An incisive measure of comprehending a region's response to storm-tide and pluvial flooding. *Environ. Res. Lett.* **2020**, *15*, 064029. [CrossRef]
37. Yu, H.; Shen, Y.; Kelly, R.M.; Qi, X.; Wu, K.; Li, S.; Yu, H.; Bao, X. Trends in social vulnerability to storm surges in Shenzhen, China. *Nat. Hazards Earth Syst. Sci.* **2020**, *20*, 2447–2462. [CrossRef]
38. Choudhury, M.-U.-I.; Haque, C.E.; Hostetler, G. Transformative learning and community resilience to cyclones and storm surges: The case of coastal communities in Bangladesh. *Int. J. Disaster Risk Reduct.* **2021**, *55*, 102063. [CrossRef]
39. Kantamaneni, K.; Panneer, S.; Sudha Rani, N.N.V.; Palaniswamy, U.; Bhat, L.D.; Jimenez-Bescos, C.; Rice, L. Impact of Coastal Disasters on Women in Urban Slums: A New Index. *Sustainability* **2022**, *14*, 3472. [CrossRef]
40. Bernard, A.; Long, N.; Becker, M.; Khan, J.; Fanchette, S. Bangladesh's vulnerability to cyclonic coastal flooding. *Nat. Hazards Earth Syst. Sci.* **2022**, *22*, 729–751. [CrossRef]
41. Ghosh, S.; Mistri, B. Cyclone-induced coastal vulnerability, livelihood challenges and mitigation measures of Matla–Bidya inter-estuarine area, Indian Sundarban. *Nat. Hazards* **2023**, *116*, 3857–3878. [CrossRef] [PubMed]
42. Zhao, Y.; Liu, Q.; Huang, R.; Pan, H.; Xu, M. Recent Evolution of Coastal Tidal Flats and the Impacts of Intensified Human Activities in the Modern Radial Sand Ridges, East China. *Int. J. Environ. Res. Public Health* **2020**, *17*, 3191. [CrossRef]
43. Cui, Y.; Yan, F.; He, B.; Ju, C.; Su, F. Characteristics of shoreline changes around the South China Sea from 1980 to 2020. *Front. Mar. Sci.* **2022**, *9*, 1005284. [CrossRef]
44. Gao, Y.; Wang, H.; Liu, G.M.; Sun, X.Y.; Fei, X.Y.; Wang, P.T.; Lv, T.T.; Xue, Z.S.; He, Y.W. Risk assessment of tropical storm surges for coastal regions of China. *J. Geophys. Res. Atmos.* **2014**, *119*, 5364–5374. [CrossRef]
45. Zhang, C.; Yin, K.; Shi, X.; Yan, X. Risk assessment for typhoon storm surges using geospatial techniques for the coastal areas of Guangdong, China. *Ocean. Coast. Manag.* **2021**, *213*, 105880. [CrossRef]
46. Wang, Y.; Chen, X.; Wang, L. Differential Semi-Quantitative Urban Risk Assessment of Storm Surge Inundation. *ISPRS Ann. Photogramm. Remote Sens. Spat. Inf. Sci.* **2022**, *10*, 177–185. [CrossRef]
47. Li, K.; Li, G.S. Vulnerability assessment of storm surges in the coastal area of Guangdong Province. *Nat. Hazards Earth Syst. Sci.* **2011**, *11*, 2003–2010. [CrossRef]
48. Li, K.; Li, G.S. Risk assessment on storm surges in the coastal area of Guangdong Province. *Nat. Hazards* **2013**, *68*, 1129–1139. [CrossRef]

49. Hatzikyriakou, A.; Lin, N. Impact of performance interdependencies on structural vulnerability: A systems perspective of storm surge risk to coastal residential communities. *Reliab. Eng. Syst. Saf.* **2016**, *158*, 106–116. [CrossRef]
50. Abdrabo, K.I.; Kantoush, S.A.; Esmaiel, A.; Saber, M.; Sumi, T.; Almamari, M.; Elboshy, B.; Ghoniem, S. An integrated indicator-based approach for constructing an urban flood vulnerability index as an urban decision-making tool using the PCA and AHP techniques: A case study of Alexandria, Egypt. *Urban Clim.* **2023**, *48*, 101426. [CrossRef]
51. Bathi, J.; Das, H. Vulnerability of Coastal Communities from Storm Surge and Flood Disasters. *Int. J. Environ. Res. Public Health* **2016**, *13*, 239. [CrossRef] [PubMed]
52. Pastor-Escuredo, D.; Morales-Guzmán, A.; Torres-Fernández, Y.; Bauer, J.-M.; Wadhwa, A.; Castro-Correa, C.; Romanoff, L.; Lee, J.G.; Rutherford, A.; Frias-Martinez, V.; et al. Flooding through the lens of mobile phone activity. In Proceedings of the IEEE Global Humanitarian Technology Conference (GHTC 2014), San Jose, CA, USA, 10–13 October 2014; IEEE: Piscataway, NJ, USA, 2014. [CrossRef]
53. Toya, H.; Skidmore, M. Cellular Telephones and Natural Disaster Vulnerability. *Sustainability* **2018**, *10*, 2970. [CrossRef]
54. Guo, J.; Song, W.; Zheng, H. Assessment of Comprehensive Fishery Loss due to Storm Surge Based on Modified Order Relation Weighting Model. *J. Coast. Res.* **2020**, *104*, 541–545. [CrossRef]
55. Wang, L.; Hu, S.; Han, J.-C.; Hu, P.; Yu, X. Mitigation measures of storm surge inundation at an onshore aquaculture farm. *J. Hydrol.* **2024**, *638*, 131443. [CrossRef]
56. Phillips, B.F.; Pérez-Ramírez, M. (Eds.) *Climate Change Impacts on Fisheries and Aquaculture*; John Wiley & Sons, Ltd: Hoboken, NJ, USA, 2017. [CrossRef]
57. United Nations Office for Disaster Risk Reduction. Sendai Framework for Disaster Risk Reduction 2015–2030. *UNDRR*. 2015. Available online: https://www.undrr.org/publication/sendai-framework-disaster-risk-reduction-2015-2030 (accessed on 29 June 2025).
58. Disaster Resilience Scorecard for Cities | Making Cities Resilient. *Mcr2030.Undrr.org*. Available online: https://mcr2030.undrr.org/disaster-resilience-scorecard-cities (accessed on 25 August 2021).
59. APEC Integrated Urban Planning Report–Combining Disaster Resilience with Sustainability | APEC. *APEC*. 2025. Available online: https://www.apec.org/Publications/2021/03/APEC-Integrated-Urban-Planning-Report (accessed on 29 June 2025).
60. Urban Socio-Economic Survey Department of the National Bureau of Statistics. In *China Urban Statistical Yearbook 2021*; Xu, L., Ed.; China Statistics Press: Beijing, China, 2022. (In Chinese)
61. National Marine Data and Information Service. In *Tide Table*; Lu, Y., Ed.; China Ocean Press: Beijing, China, 2019; Volume 1–3. (In Chinese)
62. China Standardization Committee. *Guideline for Risk Assessment and Zoning of Storm Surge Disaster*; China Quality Inspection Press: Beijing, China, 2020; pp. 22–24. Available online: https://max.book118.com/html/2018/0830/7053131031001145.shtm (accessed on 29 June 2025). (In Chinese)
63. Gornitz, V. Global coastal hazards from future sea level rise. *Glob. Planet. Chang.* **1991**, *89*, 379–398. [CrossRef]
64. Hammar-Klose, E.S.; Thieler, E.R. *Coastal Vulnerability to Sea-Level Rise: A Preliminary Database for the U.S. Atlantic, Pacific, and Gulf of Mexico Coasts*; Data Series; U.S. Geological Survey: Reston, VA, USA, 2001. [CrossRef]

Disclaimer/Publisher's Note: The statements, opinions and data contained in all publications are solely those of the individual author(s) and contributor(s) and not of MDPI and/or the editor(s). MDPI and/or the editor(s) disclaim responsibility for any injury to people or property resulting from any ideas, methods, instructions or products referred to in the content.